Desalination and Water Treatment
www.deswater.com
1944-3994/1944-3986 © 2009 Desalination Publications. All rights reserved

7 (2009) 12–17

Properties of amino-functionalized silica membranes for the dehydration of water/ethanol mixtures

Sadao Araki[a,b*], Tatsuya Satoh[b], Hayato Doi[b], Hiroyuki Yano[b], Yoshikazu Miyake[b,c]

[a]*Business Promotion and Product Development Center, Technical Research Institute, Hitachi Zosen Corporation,*
2-11, Funamachi 2-chome Taisho-Ku, Osaka 551-0022, Japan
Tel. +81 6 6551 9173; Fax: +81 6 6551 9841; emal: araki.sa@gmail.com
[b]*Department of Chemical Engineering;* [c]*High Technology Research Center, Kansai University,*
3-35, Yamatecho 3-chome, Suita 564-8680, Japan

Received 1 July 2008; Accepted 16 March 2009

ABSTRACT

Amino-functionalized silica membranes were applied to the separation of water/ethanol mixtures by pervaporation. An increased interaction between the silica membrane surface and permeating materials is important in order to enhance separation. In this study, the improvement in water permeance ability and selectivity was examined by modifying the silica membrane surface with amino groups. Silica membranes were prepared by the sol-gel method of hydrolysis and co-condensation processes using tetraethoxysilane (TEOS) as a silica source and 3-aminopropyltriethoxysilane (APTES) to introduce the amino groups. The performance of membranes prepared with various molar ratios of TEOS/APTES was evaluated by pervaporation of water/ethanol. The separation property of the amino-functionalized membrane was higher than that of a membrane prepared with TEOS. The membranes were characterized by FE-SEM, FT-IR and single gas permeation measurements of He and N_2.

Keywords: Pervaporation; Silica membrane; Amino group; Hydrophilicity; Dehydration

---

1. Introduction

Pervaporation and vapor permeation are very attractive separation technologies for many aqueous solutions of organic solvent with an azeotropic point. Pervaporation is a separation process in which one component of the mixture is separated by selective evaporation through the membrane. The driving force for mass transport of permeating materials from feed mixture is the difference of the chemical potential of permeating material across the membrane. The difference of the chemical potential can be created by using vacuum pump or sweep gas on the permeate side to maintain the chemical potential of the permeate side lower than the feed side [1]. As the separation of the mixture can be carried out by the difference of the chemical potential, the energy consumption of these separation technologies is lower than the commercialized distillation process [1–4]. The organic polymer membranes generally used in these pervaporation processes show high selectivity. However, the drawbacks of these membranes are small flux owing to low separation temperature for their thermal stability, and membrane swelling with organic solvent [4–6]. On the other hand, inorganic membranes possess highly chemical and ther-mal stabilities. An asymmetric silica membrane consisting of an α-alumina support and a γ-alumina interlayer has been used as a typical ceramic membrane. The good performance in the dehydration of an alcohol/water solution using a silica membrane is due to the interaction of water with the surface silanol group of the silica [6–10]. Betten et al. reported the transport mechanisms of pure components in pervaporation through

---

*Corresponding author.

microporous silica membrane [11]. They concluded in the report that flux could not be correlated with size parameters such as molecular weight, kinetic diameter and effective diameter, and that there was an exponential relationship between the Hansen polarity and the flux. This result suggests that the interaction between the silica membrane surface and permeating materials is important in order to enhance separation.

On the other hand, there has been an increase of research into the chemical functionalization of silica surface attention due to afford the adsorbent tailored to the application such as catalyst [12], gas separation media [13,14], and the other research [15–17]. One of these studies, Wu et al., reported that silica surface modified a small amount of APTES led to an increase of water adsorption [18].

In this study, the improvement in the water permeance ability and selectivity of a silica membrane was examined by modifying the silica membrane surface with amino groups. Silica membranes were prepared by the sol-gel method, which consists of the hydrolysis and co-condensation processes using tetraethoxysilane (TEOS) as a silica source and 3-aminopropyl-triethoxysilane (APTES) to introduce the amino groups. The performance of the silica membranes prepared with various molar ratios of TEOS/APTES was evaluated by pervaporation of water/ethanol.

2. Experimental

Amino-functionalized silica membranes were prepared by dip-coating used the sol-gel method on an α-alumina support with a γ-alumina interlayer. The structure of the α-alumina support and preparation of the interlayer have been described in another paper [19]. The γ-alumina interlayers were prepared by dipping α-alumina tubes into a Boehmite (γ-AlOOH) sol. The outside of the α-alumina tubes was dip-coated in 0.6 mol l^{-1} Boehmite solution for 10 s, dried at room temperature for 3 h, and then calcined at 600°C for 3 h (heating and cooling rate; 1°C min^{-1}).

Amino-functionalized silica membranes were prepared by dip-coating them in a sol consisting of TEOS and APTES (APTES=0, 50, 75, 90, 100 mol%, denoted as M-0, M-50, M-75, M-90, M-100, respectively). The 1.0 mol prescribed amounts of TEOS and APTES were added into 25 ml of ethanol with gentle stirring. 1 N HNO_3 was delivered slowly by drops into the mixture and continuously stirred at room temperature for 10 min. The temperature of the mixture was raised to about 70°C and refluxed for 150 min. The resulting sol was diluted to 0.1 mol l^{-1} as a silica source by ethanol. The α-alumina support with a γ-alumina interlayer was dipped into the sol and dried at room temperature for 3 h. Subsequently, the membranes were aged at 80°C for 3 h.

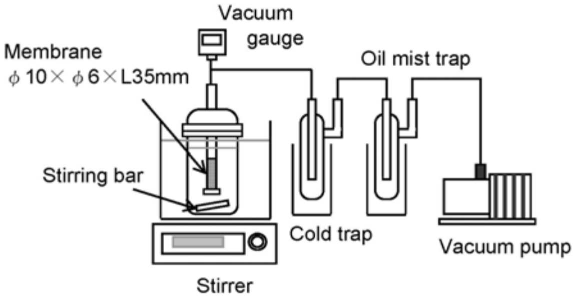

Fig. 1. Schematic diagram of the apparatus for pervaporation.

The chemical structure of the sol after refluxing was characterized by FT-IR spectroscopy. The sol used for the measurement was dried at room temperature and aged at 80°C. FE-SEM was used to study the surface and cross-sectional and morphological structures of the amino-functionalized silica membrane. Samples were prepared by mechanically breaking the membranes, and coating them with a layer of osmium by osmium coater (Neoc-ST, Meiwafosis, Japan).

To estimate the porosity of membranes, single gas permeation experiments were performed at room temperature. The pressures of the support and membrane sides were maintained at 200 kPa and ambient pressure, respectively. The permeation flow through the membrane under the pressure drop across the membrane was measured using a bubble flow meter.

Pervaporation experiments were performed at 30°C, as shown in Fig. 1. A tubular membrane with a closed-end structure was placed in a 500 ml glass vessel. This vessel was filled with water/ethanol mixture, and the mixture was mixed by a stirrer bar. The pressure of the permeate side, provided by a vacuum pump, was about 40 Pa. The permeated vapor was collected by a liquid nitrogen cold trap. The permeate pressure was measured by Pirani vacuum gauges (GP-1000G, Alvac). The water concentrations of feed and permeate sides were measured by Karl-Fisher titration (MKS-500, Kyoto Electronics Manufacturing, Japan).

3. Results and discussion

3.1. Characterization of amino-functionalized silica membranes

Fig. 2 shows the FT-IR spectra of silica (M-0) and amino-functionalized silica membranes (M-75, M-100). A strong and broad band at around 3400 cm^{-1} corresponding to O-H stretching vibrations of the hydroxyl groups appeared in the spectra for all membranes. The presence of amino groups is indicated by the presence of vibrations for N-H asymmetric stretching at 3353 cm^{-1}, N-H symmetric stretching at 3262 cm^{-1}, the overtone of N-H deformation at 3175 cm^{-1} and N-H primary amine deformation at 1585 cm^{-1} [20–23]. Regarding the amino-functionalized membranes, these typical adsorption bands of amino groups were observed. The increase in the intensity of the adsorption bands at 2965 and 2911 cm^{-1} for CH_2 asymmetric stretching and CH_2 symmetric stretching, respectively, showed the CH_2 of the aminopropyl groups of APTES. The strength of these peaks in M-75 was decreased compared with that of M-100, due to the lower amount of APTES. However, these results indicated the presence of amino groups in the amino-functionalized membrane.

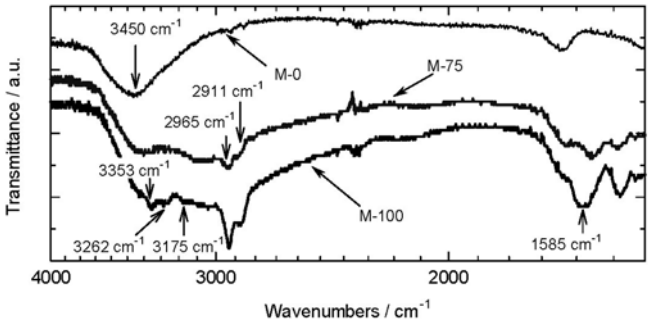

Fig. 2. FT-IR spectra of silica and amino-functionalized silica membranes.

FE-SEM was carried out to compare the morphology of the silica and amino-functionalized membranes. The cross-sectional images and surface images obtained by FE-SEM are shown in Fig. 3. FE-SEM images of the surfaces of silica and amino-functionalized silica membranes are shown in Fig. 3(a)–(c). The surface of the silica membrane was almost smooth with little projection, as shown in Fig. 3(a). The surface of the amino-functionalized membrane, which had been introduced to 75mol% APTES (M-75), presented some projection, but was almost smooth similar to M-0. Compared with the surfaces of M-0 and M-75, the surface image of amino-functionalized membrane prepared with only APTES (M-100) was rough and irregular, and was observed large pore such as cracks or

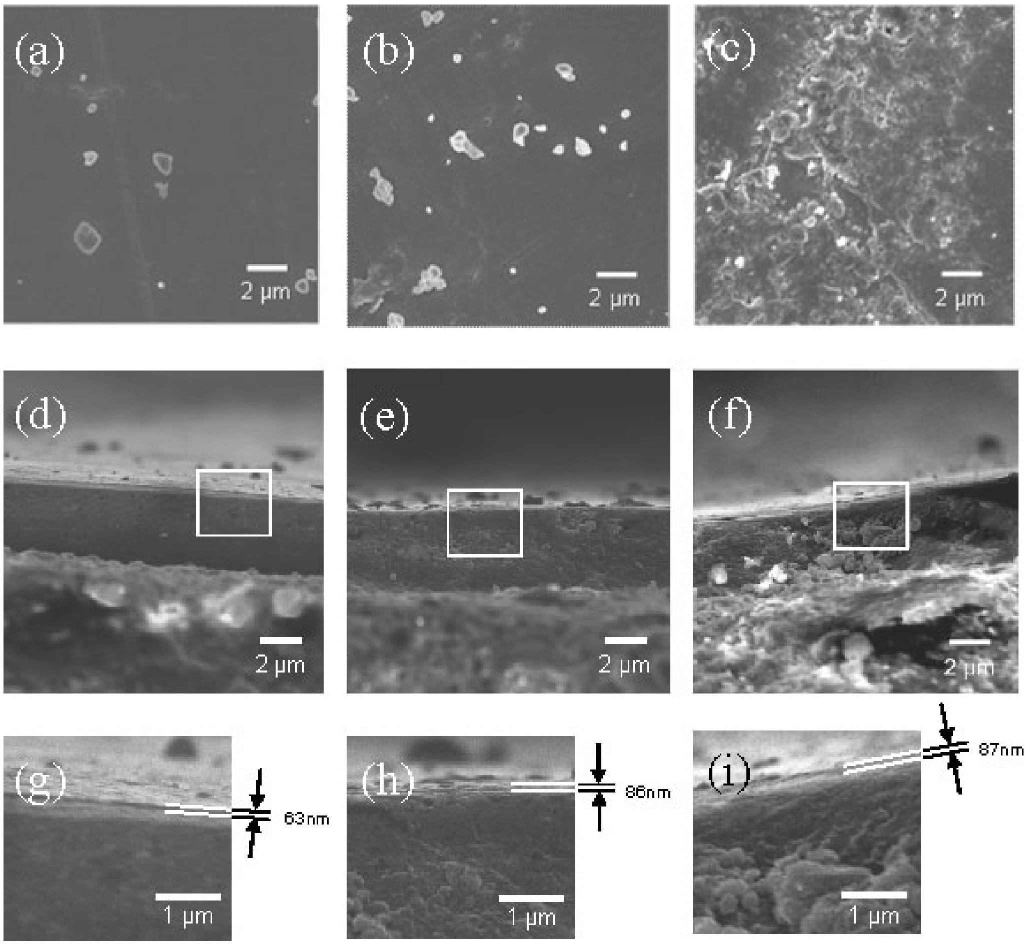

Fig. 3. FE-SEM images of a silica membrane: (a) surface of M-0, (b) surface of M-75, (c) surface of M-100, (d) cross-section through M-0, (e) cross-section through M-75, (f) cross-section through M-100, (g) magnified image for the portion of the box in (d), (h) magnified image for the portion of the box in (e), (i) magnified image for the portion of the box in (f).

pinholes. The condition that prepared by only APTES as silica source is not suitable because the bounding site of APTES is one fewer than that of TEOS. As a result, it is considered that silica networks are nonuniformly formed due to concentration of aminopropyl group in surface. In addition, this result might be led by the viscosity difference of silica sol for dip coating because of the faster condensation rate of the organo-silane precursors with amino groups [24,25]. Thus, the APTES content in silica source has the suitable condition for the preparation of membranes.

The supports consisted of α-alumina coated with the γ-alumina layer, as observed in the FE-SEM images in Fig. 3(d)–(i). Fig. 3(g)–(i) is the magnified images for the portion of the box in Fig. 3(d)–(f). The thickness of the γ-alumina layer is 3.5–4.0 μm. The thicknesses of M-0, M-75 and M-100 are 63 nm, 86 nm and 87 nm, respectively. These measurements were carried out at local point and there is some uncertainty in the regard to the overall membrane thickness. There was not much difference among these membranes. However this result showed the tendency that amino-functionalized silica membrane is thicker than silica membrane. Meanwhile, the thickness between M-75 and M-100 made no difference.

To estimate the porosity of the membranes, single gas permeation experiments for He and N_2 were performed at room temperature. Fig. 4 shows He permeance and α (He/N_2) reflecting the influence of APTES content. α(He/N_2) represents the ratio of He permeance to N_2 permeace, which is measured by single gas permeation experiments for each gas. α (He/N_2) indicated selectivity similar to Knudsen diffu-sion. Other research reported that the typical silica mem-brane indicated high selectivity compared to Knudsen diffusion due to uniform microporous structure under a kinetic diameter of 0.364 nm for N_2 and 0.38 nm for methane [6,19]. However, the silica membranes in this research might have a broad pore distribution. In this study, the silica membrane is calcined at low temperature to prevent the decomposition of the hydroxyl and amino group. One reason is the difference in the calcination process relative to other research. The He permeance of silica membranes without APTES was shown to be 1.0×10^{-6} mol m^{-2} s Pa. He permeance is found to decrease with increasing APTES content reaching a minimum at 75mol% of APTES content. The membrane of 75mol% APTES (M-75) showed the lowest He permeance; 1.4×10^{-9}mol m^{-2}. As He permeance is expected the relation with the membrane thickness, it is considered that this decrease is confirmed by the increasing tendency of membrane thickness of M-75 compare with that of M-0. However, He permeance of M-75 is almost three orders of magnitude slower than that of M-0. Hence, the explanation of this result is not satisfied only by the membrane thickness. It is suggested that diffusional resistance of He molecule through the membrane increased by increasing of density of the silica membranes containing APTES due to the aminopropyl group of APTES. Additionally, He permeance increases with APTES content above an APTES content of 75mol%. Because, as shown in Fig.3, pinholes or cracks were observed in membranes with high APTES content, it can be concluded that the optimum condition for preparation of an amino-functioned silica membrane is 75mol% of APTES.

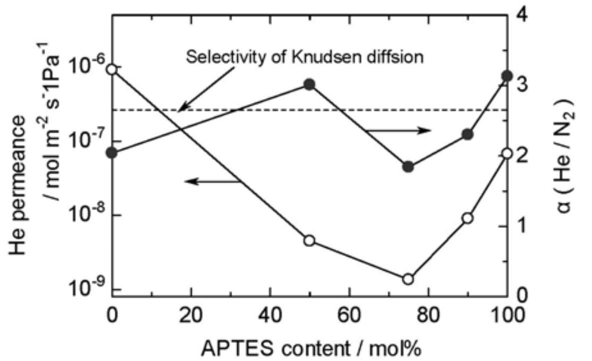

Fig. 4. Effect of the APTES content of amino-functionalized silica membranes on He permeance and α (He/N_2).

3.3. Pervaporation of amino-functionalized silica membrane

The water flux and separation factor under 5%water content in feed are shown as a function of the APTES content of amino-functionalized silica membranes in Fig. 5. The separation factor of membranes is generally defined as the ratio between the concentrations of components *i* and *j* on the permeate side, relative to those on the feed side, as follows

$$\alpha = \frac{(y_i/x_i)}{(y_j/x_j)} \tag{1}$$

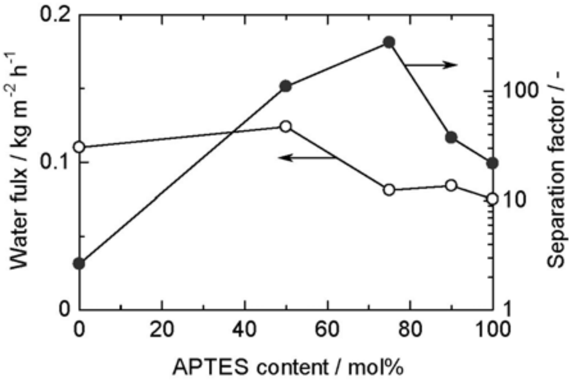

Fig. 5. Effect of the APTES content of amino-functionalized silica membranes in 5 wt% feed water at 30°C on water flux and the separation factor.

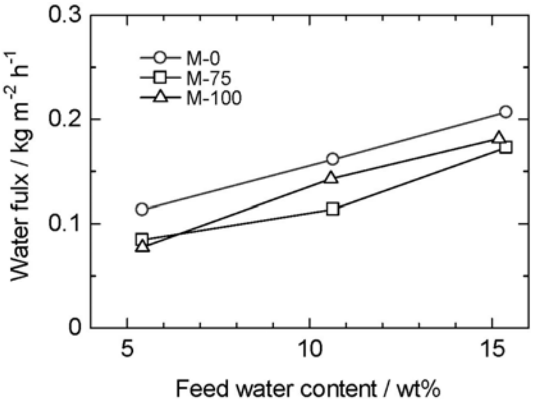

Fig. 6. Effect of the feed water content on water flux.

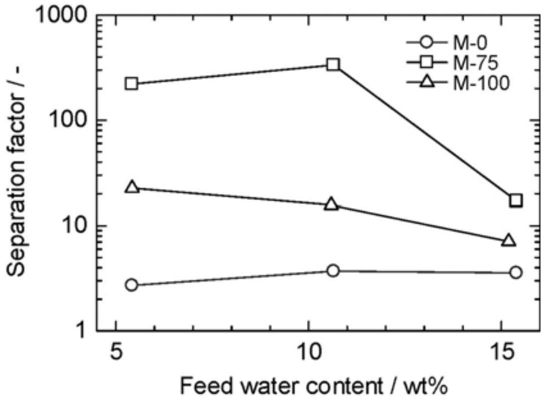

Fig. 7. Effect of the feed water content on separation factor.

where *y* and *x* are the fractions of components *i* and *j* in the permeate and feed side, respectively. In this experiment, *i* and *j* are water and ethanol, respectively. The pervaporation measurements were carried out at 30°C. Water fluxes of M-0 and M-50 are nearly constant at 0.12–0.11 kg m^{-2} h^{-1}. On the other hand, M-75, M-90 and M-100 showed water fluxes of 0.07–0.08 kg m^{-2} h^{-1}, regardless of the APTES content. The permeation mechanisms through the membrane is considered the adsorption and diffusion model, which consists of the adsorption of permeate materials onto the membrane surface, the diffusion of permeate material through micropores and desorption of permeate materials from the membrane. Therefore, the water flux should be affected by the membrane thickness, porosity of membrane and interactions between membrane and permeate materials [11,26–28]. In Fig. 3(g)–(i), the amino-functionalized membrane is slightly thicker than the silica membrane. However, the amino-functionalized membranes are of low porosity compared with the silica membrane due to the aminopropyl group, the minimum of He permeance reached at M-75. Therefore, water flux across the amino-functionalized membrane might be prevented by the thicker membrane thickness and the decrease in porosity.

On the other hand, the optimal value of the separation factor was observed, and when APTES was 75mol%, the highest value of 280 was indicated. This result suggested that the membrane containing APTES 75mol% was prepared uniformly by the sol mixed of TEOS and APTES.

The effects of the feed water content on water flux and separation factor are shown in Figs. 6 and 7, respectively. Several feed water concentrations between 5 wt%–15 wt% were tested at 30°C. With a high water content (15 wt%), the water fluxes across membranes were 0.17–0.2 kg m^{-2} h^{-1}. The water flux increased almost linearly with increases in water content in the feed. No difference in water flux across the membrane was observed, even though the water concentration in the feed varied. Separation factors greatly depend on the APTES contents in membrane, and the values for M-75 were the highest. Except for the silica membrane, the separation factor for amino-functionalized membranes with 15wt% feed water content was minimal. The decrease in separation factor with high water concentration can be explained by the drag effect, which in turn is explained by the Maxwell-Stefan theory [10,29,30]. In brief, ethanol is not sufficiently polar to be adsorbed onto the membrane. However, if water is significantly present, ethanol molecules are surrounded by the water molecules. As a result, ethanol can permeate through the membrane against its own concentration gradient [30].

4. Conclusions

Silica membranes were prepared by the sol-gel method of hydrolysis and co-condensation processes with TEOS as a silica source and APTES to introduce amino groups. The separation property of the amino-functionalized membrane of 75 mol% of APTES was higher than that of the membrane prepared by TEOS, with a separation factor of 280 for the APTES 75 mol% membrane compared with that of the silica membrane. FE-SEM surface images of this amino-functionalized membrane (M-75) indicated a smooth surface, suggesting good compatibility between TEOS and APTES. Moreover, M-75 was found to show the lowest He permeance of 1.4×10^{-9} mol m^{-2}, and the highest density out of all of the membranes, presumably due to the aminopropyl group of APTES. The reason that a high separation property was achieved might be an increase in the interactions between the silica membrane surface and permeating materials due to the introduction of APTES with an amino-group, producing a uniformly dense membrane without pinholes or cracks.

References

[1] X. Feng and R.Y.M. Huang, Liquid separation by membrane pervaporation: A review, Ind. Eng. Chem. Res., 36 (1997) 1048.

[2] J. Sekelic, J.E. ten Elshof and D.H.A. Blank, Separation mechanism in dehydration of water/organic binary liquids by pervaporation through microporous silica, J. Membr. Sci., 254 (2005) 267.

[3] T.A. Peters, J. van der Tuin, C. Houssin, M.A.G. Vorstman, N.E. Benes, Z.A.E.P Vroon, A. Holmen and J.T.F. Keurentjes, Preparation of zeolite-coated pervaporation membranes for the integration of reaction and separation, Catalysis Today, 104 (2005) 288.

[4] H.M. van Veen, Y.C. van Delft, C.W.R. Engelen and P.P.A.C. Pex, Dewatering of organics by pervaporation with silica membranes, Sep. Purif. Meth., 22–23 (2001) 361.

[5] M. Asaeda, J. Yang and Y. Sakou, Porous silica-zirconia (50%) membranes for pervaporation of iso-propyl alchol (IPA)/water mixtures, J. Chem. Eng. Japan, 35 (2002) 365.

[6] T.A. Peters, J. Fontalvo, M.A.G. Vorstman, N.E. Benes, R.A. van Dam, Z.A.E.P Vroon, E.L.J. van Soest-Vercammen and J.T.F. Keurentjes, Hollow fiber microporous silica membrane for gas separation and pervaporation: Synthesis, performance and stability, J. Membr. Sci., 248 (2005) 73.

[7] R.W. van Gemert and F.P. Cuperus, Newly developed ceramic membranes for dehydration and separation of organic mixtures by pervaporation, J. Membr. Sci., 105 (1995) 287.

[8] C. Casado, A. Urtiaga, D. Gorri and I Ortiz, Pervaporative dehydration of organic mixtures using a commercial silica membrane Determination of kinetic parameters, Sep. Purif. Technol., 42 (2005) 39.

[9] A.W. Verkerk, P. van Male, M.A.G. Vorstman and J.T.F. Keurentjes, Properties of high flux ceramic pervaporation membranes for dehydration of alchol/water mixtures, Sep. Purif. Technol., 22–23 (2001) 689.

[10] A.W. Verkerk, P. van Male, M.A.G. Vorstman and J.T.F. Keurentjes, Description of dehydration performance of amorphous silica pervaporation membranes, J. Membr. Sci., 193 (2001) 227.

[11] B. Bettens, S. Dekeyzer, B.V. der Bruggen, J. Degreve and C. Vandecasteele, Transport of pure component in pervaporation through a microporous silica membrane, J. Phys. Chem. B, 109 (2005) 5216.

[12] X. Wang, C. Chen, S. Chen and Y. Mou, Arenesulfonic acid functionalized mesoporous silica as a novel acid catalyst for the liquid phase Beckmann rearrangement of cyclohexanone oxime to epsilon-caprolactam, Appl. Catal., A 281 (2005) 47.

[13] Y. Sakamot, K. Nagata, K. Yogo and K. Yamada, Preparation and CO_2 separation properties of amine-modified mesoporous silica membranes, Micropor. Mesopor. Mater., 101 (2007) 303.

[14] G.P. Knowles, J.V. Graham, S.W. Delaney and A.L. Chaffee, Aminopropyl-functionalized mesoporous silicas as CO_2 adsorbents, Fuel Processing Technol., 86 (2005) 1435.

[15] S. Reculusa, P. Massé and S. Ravaine, Three-dimensional colloidal crystals with a well-defined architecture, J. Coll. Interf. Sci., 279 (2004) 471.

[16] L. Bois, A. Bonhommé, A. Ribes, B. Pais, G. Raffin and F. Tessier, Functionalized silica for heavy metal ions adsorption, Coll. Surf., A 221 (2003) 221.

[17] B. Lee, Y. Kim, H. Lee and J. Yi, Synthesis of functionalized porous silicas via templating method as heavy metal ion adsorbents: the introduction of surface hydrophilicity onto the surface of adsorbents, Micropor. Mesopor. Mater., 50 (2001) 77.

[18] Z. Wu, H. Xiang, T. Kim, M.S. Chun and K. Lee, Surface properties of submicrometer silica spheres modified with aminopropyltriethoxysilane and phenyltriethoxysilane, J. Coll. Interf. Sci., 304 (2006) 119.

[19] S. Araki, N. Mohri, Y. Yoshimitsu and Y. Miyake, Synthesis, characterization and gas permeation properities of a silica membrane prepared by high-pressure chemical vapor deposition, J. Membr. Sci., 290 (2007) 138.

[20] J. Kim, D. Jung, Y. Park, Y. Kim, D. won Moon and T.G. Lee, Quantitative analysis of surface amine groups on plasma-polymerized ethylenediamine films using UV–visible spectroscopy compared to chemical derivatization with FT-IR spectroscopy, XPS and TOF-SIMS, Appl. Surf. Sci., 253 (2007) 4112.

[21] A. Choukourov, H. Biederman, I. Kholodkov, D. Slavinska, M. Trchova and A. Hollander, Properties of amine-containing coatings prepared by plasma polymerization, J. Appl. Polym. Sci., 92 (2004) 979.

[22] A.T. Bell, T. Wydeven and C.C. Johnson, A study of the performance and chemical characteristics of composite reverse osmosis membranes prepared by plasma polymerization of allylamine, J. Appl. Polym. Sci., 19 (1975) 1911.

[23] R.C. Ruaan, T.-H. Wu, S.-H. Chen and J.-Y. Lai, Oxygen/nitrogen separation by polybutadiene/polycarbonate composite membranes modified by ethylenediamine plasma, J. Membr. Sci., 138 (1998) 213.

[24] M.C. Burleigh, M.A. Markowitz, M.S. Spector and B.P. Gaber, Amine-functionalized periodic mesoporous organosilicas, Chem. Mater., 13 (2001) 4760.

[25] M.C. Burleigh, M.A. Markowitz, M.S. Spector and B.P. Gaber, Direct synthesis of periodic mesoporous organosilicas: functional incorporation by co-condensation with organosilanes, J. Phys. Chem., B 105 (2001) 9935.

[26] J.G. Wijmans and R.W. Baker, A simple predictive treatment of the permeation process in pervaporation, J. Membr. Sci, 79 (1993) 101.

[27] D. Shah, K. Kissick, A. Ghorpade, R. Hannah and D. Bahattacharyya, Pervaporation of alcohol-water and dimethylformaide-water mixtures using hydrophilic Zeolite NaA membranes: mechanisms and experimental results, J. Membr. Sci., 179 (2000) 185.

[28] T.C. Bowen, S. Li, R.D. Noble and J.L. Falconer, Driving force for pervaporation through Zeolite membranes, J. Membr. Sci., 225 (2003) 165.

[29] J. Sekulć, J.E. ten Elshof and D.H.A. Blank, Separation mechanism in dehydration of water/organic binary liquids by pervaporation through microporous silica, J. Membr. Sci., 254 (2005) 267.

[30] B. Bettens, J. Degrève, B.V. der Bruggen and C. Vandecasteele, Transport of binary mixtures in pervaporation through a microporous silica membrane: Shortcomings of Fickian models, Sep. Sci. Technol., 42 (2007) 1.